Transportation Research Part C 180 (2025) 105309

Contents lists available at ScienceDirect

Transportation Research Part C

journal homepage: www.elsevier.com/locate/trc

Communication-free Distributed Control Algorithm for autonomous vehicles at intersections

Alireza Soltani, David M. Levinson, Mohsen Ramezani *

The University of Sydney, School of Civil Engineering, Sydney, NSW 2006, Australia

ARTICLE INFO

Keywords:
Automated vehicles
Signal-free intersection
Distributed systems
Decentralized agent
Deadlock prevention

ABSTRACT

This paper introduces a novel approach for managing autonomous vehicles at signal-free intersections through a *Communication-free Distributed Control Algorithm* (CfDCA). Unlike centralized systems or communication-based decentralized methods, CfDCA relies solely on onboard sensors and in-vehicle decision-making to ensure efficient and collision-free navigation. The algorithm formulates intersection management as a distributed optimization problem with demonstrated safety logics and robustness to measurement errors. The algorithm combines a dynamic resource acquisition graph with a refined priority function and an adaptive tolerance mechanism to ensure efficient performance under varying traffic conditions. A stochastic tie-breaking mechanism is proposed to handle rare cases of identical priorities, while deadlock prevention is guaranteed through strict priority ordering. Simulation experiments demonstrate that CfDCA reduces average delay and queue length and is able to achieve throughput higher than actuated signalized intersections and outperforms a first-come-first-served baseline in delay reduction. Additionally, the algorithm's distributed design offers scalability and eliminates dependency on communication infrastructure.

1. Introduction

1.1. Background

Traditional urban traffic control systems, including traffic signals, roundabouts, and stop signs, have long been the cornerstone of intersection management. However, the emergence of Autonomous Vehicles (AVs) has prompted a reassessment of these conventional methods. AVs, equipped with advanced sensing and control capabilities, can achieve higher precision and reliability compared to human-driven vehicles. By following predictable trajectories and responding rapidly to dynamic traffic conditions, AVs present significant opportunities to reduce delays and improve the overall throughput of intersection operations (Mahmassani, 2016; Di and Shi, 2021).

Autonomous intersection management improves traffic flow and safety by coordinating AVs without traffic signals. Two main approaches exist: one uses intersection managers to assign space–time slots for vehicles (Levin et al., 2016), while the other lets vehicles decide cooperatively using real-time V2V and V2I data (Rios-Torres and Malikopoulos, 2016). The former depends on fixed infrastructure and faces risks like communication delays and single points of failure. The latter, by leveraging AV autonomy, reduces external control, pointing towards fully self-managed intersections.

* Corresponding author.
E-mail address: mohsen.ramezani@sydney.edu.au (M. Ramezani).

https://doi.org/10.1016/j.trc.2025.105309
Received 22 February 2025; Received in revised form 13 June 2025; Accepted 13 August 2025
Available online 28 August 2025

As deployment approaches 100% AVs, it becomes feasible to implement a distributed system characterized by fully decentralized and independent decision-making processes for each AV. This decentralized approach eliminates reliance on centralized infrastructure and mitigates communication dependencies, empowering individual AVs to navigate intersections safely and efficiently. To realize this potential, it is essential to thoroughly understand the operational characteristics of intersections with AV users, particularly in terms of throughput and delay.

To this end, it is essential to understand the operational limits of intersections, particularly the interaction between conflicting movements and overall capacity. The maximum capacity of an intersection with two conflicting movements occurs when vehicles are present only in one movement, allowing crossing at maximum flow with no friction or lost time. However, as inflow from a conflicting movement increases, the capacity decreases. This principle extends to multi-legged and multi-lane intersections, where the highest throughput is achieved by maximizing the flow of the largest set of non-conflicting movements.

These dynamics underscore the critical role of conflict zones in determining intersection performance. This is especially important under high-inflow scenarios, where optimizing the sequence and timing of vehicle crossings is key to maintaining throughput while avoiding congestion.

Effective distributed conflict resolution at conflict zones must adapt to varying inflow levels, especially in intersections exclusively serving AVs. This distributed conflict resolution approach is a central component of our method, *Communication-free Distributed Control Algorithm* (CfDCA), designed to adapt to varying inflow levels. In CfDCA, each AV independently manages its interactions with conflict zones based on local sensing information. When inflow is below capacity, the focus shifts to minimizing delay by resolving conflicts efficiently, whereas at higher inflow levels, the goal becomes maximizing throughput and balancing delays across movements. This understanding forms the foundation for developing the CfDCA.

1.2. Related works

1.2.1. Centralized intersection management approaches

Research in intersection management for AVs has emphasized reservation-based protocols and the optimization of AV trajectories (Dresner and Stone, 2008). These approaches typically rely on central controllers that gather extensive data from vehicles to prioritize and optimize their movements, aiming to minimize intersection delays. For example, Dresner and Stone (2008) proposed a reservation system in which vehicle reservations are processed, and permit distribution is prioritized based on policies such as first-come-first-served (Li et al., 2013; He et al., 2018).

Alternative strategies have been proposed to prioritize vehicles. Some studies have approached permit distribution as an auction, where vehicles bid for permits, and the system allocates this limited resource to the highest bidders (Carlino et al., 2013). These systems often rely on predefined rules rather than optimizing for system-level objectives. As a result, they can lead to suboptimal performance and, in some cases, are shown to be less effective than traditional traffic signals (Levin et al., 2016; Yu et al., 2019). The concept of reservation-based rules for optimizing intersection traffic has also been extended through protocols where intersection managers assign reservations to vehicles (Levin and Rey, 2017), thereby broadening the scope for optimization.

To address these limitations, researchers have explored centralized control mechanisms to optimize intersection performance (e.g. Yang et al. (2016), Medina et al. (2019), Kamal et al. (2014) and Mirheli et al. (2019)). These efforts also highlight the potential to improve safety by reducing and mitigating traffic crashes (Rios-Torres and Malikopoulos, 2016).

1.2.2. Communication-based distributed approaches

These methods face significant practical barriers, particularly the extensive communication requirements needed for real-time implementation. Optimization-based approaches for managing signal-free intersections often enforce collision avoidance as a constraint while prioritizing operational efficiency, such as minimizing delays or maximizing throughput.

The integration of connected automated vehicle (CAV) information into intersection control strategies has been extensively studied. AV trajectories can be modified to optimize objectives such as increasing throughput and minimizing delay (e.g. Li and Wang (2006) and Lee and Park (2012)). Cooperative or distributed methods typically rely on constant communication between AVs when near an intersection, enabling them to optimize trajectories through local mutual agreements. For instance, Mirheli et al. (2019) proposed a decentralized optimization scheme in which each vehicle independently solves its own trajectory optimization problem, assuming that the decisions of other vehicles remain constant. A consensus between vehicle solutions is sought through an iterative communication process.

In less congested scenarios, decentralized or cooperative methods show promise by using direct vehicle-to-vehicle communication, but they often face real-world constraints. These approaches demand substantial bandwidth (Gholamhosseinian and Seitz, 2022). Connected vehicles require robust communication protocols and capabilities to ensure reliable operation. Limited studies, such as Makarem and Gillet (2011) and Makarem and Gillet (2012), have investigated distributed methods where AVs share basic data, such as position, speed, and path, to avoid collisions. However, these studies often rely on restrictive physical assumptions, such as very low speeds or high acceleration and deceleration capabilities, which may not hold in real-world conditions. Consequently, although collision avoidance remains the primary goal in these approaches, efficiency is often compromised as the focus shifts to navigating intersections without deadlocks or collisions.

1.2.3. Advanced control frameworks and extensions

Extending intersection management principles beyond conventional intersections, researchers have explored applications to other traffic scenarios. For instance, Mohebifard and Hajbabaie (2021) applied similar optimization concepts to single-lane roundabouts, demonstrating potential improvements in traffic flow. Similarly, Naderi et al. (2023) developed a distributed control scheme for automated vehicles on large lane-free roundabouts that relies on vehicle-specific movement corridors and nonlinear feedback controllers. However, such studies typically rely on idealized conditions, which may not account for real-world challenges such as sensor inaccuracies.

In Hao et al. (2024), a hierarchical control framework bridges optimized global trajectories and AVs' local planners to manage uncertainties and dynamic changes in real-world environments, acknowledging AVs' sophisticated local planning capabilities rather than treating them as objects following predetermined trajectories. Hao et al. (2023) introduces a lane-allocation-free intersection management method with flexible routing for connected and automated vehicles through multiple arms. Both rely on vehicle-to-vehicle or vehicle-to-infrastructure communication, creating potential vulnerabilities.

1.2.4. Communication-free approaches and research gaps

It is crucial to distinguish between different types of assumptions in existing studies. Some assumptions are fundamental to the AV domain (such as lane discipline in lane-based environments and the presence of sensing capabilities). Others create practical implementation barriers (such as requiring perfect communication, centralized control, or unrealistic vehicle dynamics). While our proposed approach shares some fundamental assumptions with existing work, it specifically targets eliminating dependencies on communication and centralized control, whereas considering real-world physical constraints on acceleration and deceleration, which represent significant practical barriers to real-world implementation. Alternative approaches, such as flexible road space allocation and model predictive control for lane-free signal-free intersections (Malekzadeh et al., 2021; Naderi et al., 2025) offer different trade-offs by allowing more flexible vehicle movement patterns but typically requiring more computational resources.

The methods above largely depend on constant or near-constant communication. To address the challenges associated with communication loss in distributed systems, recent studies have proposed strategies to maintain operational efficiency. For instance, Chen et al. (2021) introduced a cooperative cruising strategy for autonomous taxi fleets, leveraging historical trip data to optimize passenger pickups without relying on real-time communication. Their study highlights how distributed systems can function effectively in the absence of communication. To our knowledge, no previous study has considered real-time AV control at intersections in the absence of communications.

1.3. Contributions and paper structure

Centralized and communication-dependent methods face significant limitations, including the need for robust infrastructure, susceptibility to communication failures, and computational complexity of real-time optimization. These challenges highlight the necessity of a communication-free and distributed approach. Enabling each AV to navigate intersections using onboard sensors and local data independently eliminates dependency on external communication networks. This approach improves system robustness and scalability while simplifying the operational framework, making it more adaptable to varying traffic conditions and inflow levels. This underscores the need for a novel framework, such as the CfDCA, which addresses these limitations while leveraging AV capabilities.

This paper introduces the CfDCA, a method that enables AVs to navigate intersections safely and efficiently using data exclusively from their onboard sensors. The method assumes lane discipline, where each AV adheres to its designated path, simplifying conflict resolution and ensuring predictable vehicle behavior. For example, lane discipline aims to ensure that each AV strictly follows predefined paths, thereby preventing lateral maneuvers that could complicate conflict resolution. This assumption is particularly relevant as it reflects common design principles for structured intersection management, allowing the algorithm to focus on optimizing delay and throughput without accounting for complex lateral maneuvers.

The CfDCA addresses challenges arising from the absence of centralized control, such as the risk of deadlock, through strict priority ordering of vehicles. Strict priority ordering is enforced through a dynamic prioritization function, as described in later sections, ensuring predictable and collision-free vehicle movements. Moreover, CfDCA dynamically guides AVs on whether and how to proceed or adjust their speed to avoid collisions. The CfDCA achieves reduced delay and boosted throughput in both low- and high-inflow traffic conditions, all without requiring explicit or real-time communication.

To apply the CfDCA more effectively, this paper introduces a resource acquisition graph framework modeling AV–conflict zone interactions at intersections. AVs and conflict zones are vertices, with directed edges showing locally determined requirements and acquisitions based on onboard sensors. The model assumes strict lane discipline, with AVs following fixed paths to ensure clear and consistent conflict resolution.

Additionally, the CfDCA incorporates a refined priority function. The priority of each AV is calculated as the inverse of the time-to-intersection, depending on the vehicle's speed. This dynamic prioritization aims to ensure that faster-moving AVs are appropriately prioritized. Moreover, the algorithm minimizes unnecessary decelerations, thereby improving overall traffic flow efficiency.

This paper provides the theoretical framework for CfDCA, including formal mathematical demonstrations of its safety properties and deadlock prevention guarantees. Through simulations, we demonstrate CfDCA's effectiveness across varying traffic inflows and its robustness to realistic measurement errors, while comparing its performance against both actuated signalized control and first-come-first-served (FCFS) distributed approaches.

Table 1
Table of nomenclature.

Symbol	Description	Unit
a	Acceleration	m/s^2
$A(t, r_j)$	Acquisition function at time t for conflict zone r_j	–
$\mathcal{A}$	Active set, vehicles within D_1 from the intersection	–
$a_{\max}$	Maximum value of acceleration	m/s^2
$\mathcal{B}$	Buffer set, vehicles in $\mathcal{O}$ but outside $\mathcal{A}$	–
β	Sensitivity exponent of the tolerance function	–
C	A cycle in the dependency graph G	–
δ	Acceleration exponent in IDM model	–
Δt_i	Delay for each vehicle u_i	s
$d_{\max}$	Maximum value of deceleration	m/s^2
D_1, D_2	Distances upstream of the intersection Line of Entry required for CfDCA	m
$\mathcal{E}$	Set of directed edges in the graph, representing vehicle-to-conflict-zone requests	–
e_{ij}	Directed edge from vehicle u_i to conflict zone r_j	–
ϵ	Small threshold speed for prioritization	m/s
G	Graph representing the system as vertices and edges, $G = (\mathcal{V}, \mathcal{E})$	–
h	Headway	s
I	Number of vehicles in the system	–
J	Number of conflict zones inside the intersection	–
K	Maximum consecutive time steps for tie-breaking fallback	–
L	Distance for a vehicle to clear the conflict zone	m
$\mathcal{M}$	Set of movements in the intersection	–
$\mathcal{M}(i)$	Movement associated with vehicle u_i	–
$\mathcal{N}$	Vehicles that have not yet reached the conflict zone	–
$\mathcal{O}$	Observation set, vehicles within $D_2 + D_1$ from the intersection	–
$P[j, i]$	Priority matrix element, priority of u_i for r_j	–
$p(i)$	Priority function of vehicle u_i	–
Q_{acquire}	Vehicles in $\mathcal{A}$ eligible for conflict zone acquisition	–
Q_{require}	Vehicles in $\mathcal{O}$ requiring a conflict zone	–
r_j	A specific conflict zone	–
$R[j, i]$	Requirement matrix element, 1 if u_i requires r_j, 0 otherwise	–
s	Current space gap to leader vehicle	m
S_{LE}	AV's distance to intersection Line of Entry	m
S_{LC}	AV's distance to Line of Consideration	m
s^*	Desired minimum space gap to leader vehicle	m
$s_i(t)$	The state of vehicle u_i at time t	–
τ_{delay}	Minimum delay necessary to resolve a potential conflict	s
t	Current time	s
$t_{\text{actual},i}$	Actual traversal time of vehicle u_i	s
$t_{\text{min},i}$	Minimum possible traversal time of vehicle u_i	s
t_{clear}	Minimum required clearance time of the conflict zone	s
$t_{\text{clock,i}}$	Current vehicle clock time of vehicle u_i	s
$t_{\text{entry}}(i, j)$	Entry time of vehicle u_i into conflict zone r_j	s
$t_{\text{exit}}(i, j)$	Exit time of vehicle u_i from conflict zone r_j	s
T_0	Base delay tolerance constant	s
T_i	Time-to-intersection for vehicle u_i	s
$T_{\text{d}}(u_i)$	Delay tolerance of AV u_i	s
U	Set of vehicles in the system	–
u_i	A specific vehicle (u_i) in the set U	–
$\mathcal{V}$	Set of vertices in the graph	–
v	Speed	m/s
v'	Reduced speed after deceleration	m/s
$v_i(t)$	Speed of vehicle u_i at time t	m/s
$v_{\max}$	Maximum speed	m/s
$W[j, i]$	Weight matrix element, temporal feasibility of u_i entering r_j	–
$x_i(t)$	x-coordinate position of vehicle u_i at time t	m
$y_i(t)$	y-coordinate position of vehicle u_i at time t	m

The remainder of this paper is organized as follows. Section 2 introduces the CfDCA, detailing its framework and operational mechanisms, including the resource acquisition graph for AVs and conflict zones. Further, characteristics of CfDCA such as deadlock prevention and collision avoidance are discussed. The simulation model used to evaluate CfDCA is described in Section 3. Section 4 presents the results of the simulations, including a comparison between CfDCA and actuated signalized intersections and FCFS approach. Section 5 highlights the challenges and possible solutions for measurement errors, and other road users (vulnerable road users, emergency vehicles, public transit, mixed traffic) to ensure safe, efficient intersection control. Finally, the conclusions and potential future research directions are discussed in Section 6.

2. Communication-free Distributed Control Algorithm (CfDCA)

This section lays the theoretical foundation of CfDCA, encompassing the graph–matrix framework, priority function, deadlock prevention strategies, tie-breaking mechanism, and the conflict zone acquisition methodology. These components are crucial for ensuring decentralized, collision-free, and efficient navigation in diverse traffic conditions. The key parameters and symbols used throughout this paper are defined in Table 1.

2.1. Assumptions and preliminaries

CfDCA defines two critical detection lengths in each approach (described in Section 2.2.1), one guaranteeing safe passage and another increasing throughput. By classifying AVs based on their positions and relying on these positional cues, each AV adjusts its acceleration accordingly. The following subsections detail the geometric constraints and vehicle groupings that ensure safety and efficiency of CfDCA.

In addition to these spatial considerations, the CfDCA method operates under several key assumptions:

1. AVs are assumed to follow predetermined lane-based paths. This assumption is common in AV operation and simplifies conflict resolution by enabling predictable trajectories.
2. Onboard sensors are capable of reliably detecting the positions and speeds of other AVs within a designated range. While perfect sensing is not assumed, we recognize that sensor accuracy affects performance (addressed in detail in Section 5.1).
3. All AVs are assumed to strictly adhere to the CfDCA protocol, which is embedded within their driving modules, and operate independently. This assumption focuses our work on the problem among AVs rather than mixed traffic scenarios. In Section 5.2.4 we discuss the potential for mixed traffic scenarios using CfDCA for AVs.

The physical constraints employed in our model (such as maximum acceleration/deceleration values) are within realistic bounds for modern vehicles, avoiding overly idealized dynamics. Furthermore, unlike approaches requiring perfect, or any, inter-vehicle communication or centralized control, CfDCA is designed to function with only local information available through onboard sensing.

The CfDCA can be applied to any intersection for which we can define entry lines and conflict zones. To begin, we consider a generic four-legged intersection model that incorporates right turns, left turns, and straight movements within dedicated lanes to describe and test the proposed algorithm (Three-way (T) and Two-way intersections are naturally both reduced versions of this). Conflict zones are defined based on the positions and destination lanes of the vehicles. As illustrated in Fig. 1(a), a conflict zone is defined as an area within the intersection where the paths of two AVs may intersect. The size of a conflict zone is determined by the maximum size of the conflicting vehicles.

The CfDCA functions by managing conflict zone acquisitions among AVs. To ensure safety, a buffer time is established based on vehicle dynamics, which enforces a minimum clearance time for each conflict zone. This clearance time ensures that the conflict zone remains unoccupied for a specified interval, t_{clear}, between consecutive crossings by vehicles from different movements. This is the logic for collision-free operation while ensuring user comfort.

2.2. Problem formulation

Let us formally define the autonomous intersection management problem as follows. Consider set $U = \{u_1, u_2, \dots, u_i, u_k, \dots, u_I\}$ of autonomous vehicles approaching an intersection with set $R = \{r_1, r_2, \dots, r_j, \dots, r_J\}$ of conflict zones. Each vehicle u_i follows a predetermined path that traverses a subset of conflict zones $R_j \subseteq R$.

The state of vehicle u_i at time t is represented by $s_i(t) = (x_i(t), y_i(t), v_i(t))$, where $(x_i(t), y_i(t))$ denotes its position, and $v_i(t)$ its velocity. The control input for each vehicle is its acceleration $a_i(t) \in [-d_{\max}, a_{\max}]$.

The global optimization problem to minimize the delay in the intersection system can be formulated as:

$$\min_{\{a_i(t)\}_{i=1}^{I}} \sum_{i=1}^{I} \Delta t_i \tag{1}$$

$$|t_{\text{entry}}(i,j) - t_{\text{entry}}(k,j)| \geq \max\left(t_{\text{exit}}(i,j) - t_{\text{entry}}(i,j), t_{\text{exit}}(k,j) - t_{\text{entry}}(k,j)\right) + t_{\text{clear}}, \quad \forall r_j \in R, \forall u_i, u_k \in U, \mathcal{M}(u_i) \neq \mathcal{M}(u_k) \tag{2}$$

$$-d_{\max} \leq a_i(t) \leq a_{\max}, \quad \forall u_i \in U, \forall t \tag{3}$$

$$0 \leq v_i(t) \leq v_{\max}, \quad \forall u_i \in U, \forall t \tag{4}$$

Eq. (1) defines the objective function that minimizes the total delay experienced by all vehicles crossing the intersection. Here, $\Delta t_i = t_{\text{actual},i} - t_{\min,i}$ represents the delay experienced by vehicle u_i, with $t_{\text{actual},i}$ being the actual traversal time and $t_{\min,i}$ the minimum possible traversal time. Eq. (2) demonstrate collision avoidance by requiring that vehicles from different movements maintain a minimum safety gap when using the same conflict zone; $t_{\text{entry}}(i,j)$ and $t_{\text{exit}}(i,j)$ are the entry and exit times of vehicle u_i for conflict zone r_j and t_{clear} is the minimum safety gap. Eq. (3) constrains vehicle accelerations to realistic physical limits. Eq. (4) enforces speed limits to ensure vehicles operate within safe velocity ranges.

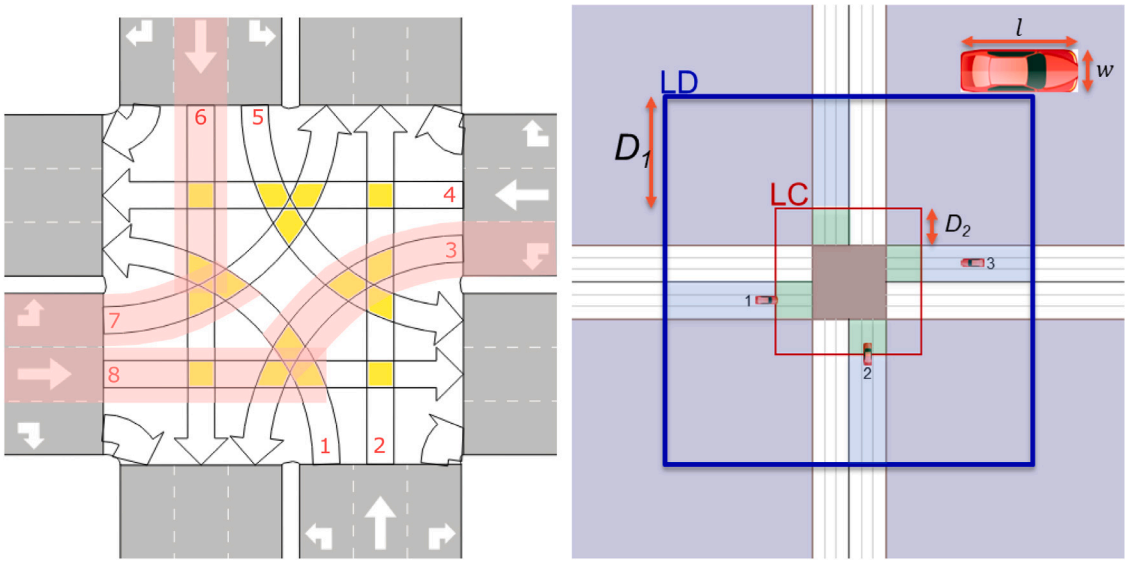

(a) (b)

Fig. 1. (a) Predefined paths and 16 conflict zones in yellow. The shaded areas with red demonstrate the spatial extent within which an AV in movement 1 monitors and evaluates other vehicles for conflict resolution. (b) Sizes and distance-based configuration of the intersection. The Line of Consideration (LC) defines the area within which AVs actively consider other vehicles for conflict zone acquisition. The Line of Detection (LD) defines the area where AVs start detecting other movements and include vehicles in the graph. AVs begin evaluating potential conflicts and requirements upon entering the LD. The colored shading illustrates the position-based vehicle sets: green areas represent the active set ($\mathcal{A}$), blue areas represent the buffer set ($\mathcal{B}$), and their combination forms the observation set ($\mathcal{O}$).

The challenge lies in solving this problem in a distributed manner, where each vehicle must make control decisions based only on local information, without centralized coordination or inter-vehicle communication. This requires decomposing the problem into locally solvable subproblems while ensuring safety constraints remain satisfied.

2.2.1. Line of detection and line of consideration

Two critical lines (Fig. 1(b)) are fundamental to the operation of the CfDCA: the Line of Detection (LD) (Thick blue) and the Line of Consideration (LC) (red). The LD is positioned at least at the safe stopping distance, denoted as D_1, upstream of the LC, and is calculated as $D_1 = \frac{v_{\max}^2}{2d_{\max}}$, where $v_{\max}$ is the maximum speed and $d_{\max}$ is the maximum deceleration. This line simply defines the minimum detection range required to achieve an efficient outcome. Li The LC is placed at a distance D_2 upstream of the intersection entry line (Eq. (5)). This line has multiple features in CfDCA. The LC serves as a decision threshold, ensuring vehicles within it are actively considered for conflict zone acquisition based on their priorities. However, when inflow is high, the graph becomes dense due to numerous conflict zone requirements, and vehicles are required to stop before reaching the LC, which prevents conflict zone acquisition while they are waiting. The CfDCA switches between low- and high-inflow regimes based on the number of AVs detected in the observation set (within $D_1 + D_2$ distance). Specifically, when the vehicle count reaches 25% of the traffic jam density within this detection zone, the system transitions to high-inflow mode, coordinating vehicle stopping positions to reduce conflicts and form platoons for sequential crossing.

Additionally, the minimum distance for D_2 is set to ensure that two conflicting vehicles, if they are approximately equidistant from the intersection, can adjust their speeds to resolve potential conflicts. To determine the minimum distance D_2 required for vehicles to cross an intersection safely, consider two vehicles approaching a conflict zone at the maximum speed $v_{\max}$. If the vehicles start to acquire conflict zones simultaneously and one begins decelerating at the maximum rate $d_{\max}$, the decelerating vehicle must add a minimum delay of τ_{delay} to its travel time to ensure safe passage. This delay can be viewed from two perspectives:

(1) From a safety perspective, $\tau_{\text{delay}} = \frac{L}{v_{\max}} + t_{\text{clear}}$, where L is the total distance required to clear the conflict zone (including the conflict zone length and the vehicle length), and t_{clear} is the safety clearance time.

(2) From a vehicle dynamics perspective, τ_{delay} is the difference between traversing distance D_2 at maximum speed versus traversing it while decelerating to a reduced speed v', where $v' = \sqrt{v_{\max}^2 - 2d_{\max}D_2}$ is the reduced speed after constant maximum deceleration over distance D_2.

Equating these two expressions yields:

$$\frac{L}{v_{\max}} + t_{\text{clear}} = \frac{2D_2}{v' + v_{\max}} - \frac{D_2}{v_{\max}}. \tag{5}$$

This equation establishes the relationship between D_2, $v_{\max}$, $d_{\max}$, L, and t_{clear}. By solving it, we determine the minimum D_2 that ensures vehicles can safely adjust their speeds to resolve conflicts while maintaining efficient traffic flow.

2.2.2. Position-based subsets

After defining D_1 and D_2 as critical distances in the CfDCA, we categorize the set of AVs (U) into subsets based on their positions relative to these distances. These position-based classifications enable each AV to independently implement distributed conflict zone management, the process by which individual AVs determine whether to proceed through or yield prior to entering the intersection without any centralized coordination. Each AV uses its onboard sensing capabilities to detect and classify nearby vehicles, creating a local representation of the traffic state that guides its decision-making.

- The set of AVs that have not yet reached the conflict zone (as exemplified by the red shaded zones in Fig. 1(a) for movement 1), is denoted as:

$$\mathcal{N} = \{u \in U \mid \text{distance}(u) > D_2 + D_1\}. \tag{6}$$

- The *observation set*, denoted as $\mathcal{O}$, includes all vehicles within a distance of $D_2 + D_1$ from the intersection entryline. This set represents the vehicles that are detectable (depicted as the combination of green and blue shaded areas in Fig. 1(b)):

$$\mathcal{O} = \{u \in U \mid \text{distance}(u) \leq D_2 + D_1\}. \tag{7}$$

- The *active set*, $\mathcal{A}$, consists of vehicles within the smaller distance of D_1. This subset includes vehicles that are closest to the intersection, requiring immediate distributed conflict zone management. Vehicles in this set are actively considered for conflict zone acquisition based on their positions and priorities (shown as green shaded areas in Fig. 1(b)):

$$\mathcal{A} = \{u \in U \mid \text{distance}(u) \leq D_1\}. \tag{8}$$

- The *buffer set*, $\mathcal{B}$, comprises vehicles in the observation set but outside the active set (illustrated as blue shaded areas in Fig. 1(b)):

$$\mathcal{B} = \{u \in \mathcal{O} \setminus \mathcal{A}\}. \tag{9}$$

  The buffer set aims to ensure vehicles that may soon enter the active set are monitored but do not immediately influence conflict zone acquisition.
- The vehicles within the observation set that require a conflict zone are given by the intersection of the observation set and the set of vehicles not yet reached the conflict zone:

$$\mathcal{Q}_{\text{require}} = \mathcal{O} \cap \mathcal{N}. \tag{10}$$

- Similarly, the vehicles within the active set that are eligible for conflict zone acquisition are defined as:

$$\mathcal{Q}_{\text{acquire}} = \mathcal{A} \cap \mathcal{N}. \tag{11}$$

Note that each AV independently detects and classifies nearby vehicles into these position-based subsets using only its onboard sensors. Autonomous vehicles are equipped with sensor suites including cameras, LiDAR, and radar with detection ranges well beyond the required distances. This sensing capability enables each AV to construct a representation of the traffic state generally consistent with other AVs in its vicinity, allowing distributed decision-making without requiring external infrastructure or vehicle-to-vehicle communication. While sensing errors may occasionally occur, they typically affect temporary speed adjustments rather than compromising safety, as discussed in Section 5.1.

2.3. Resource acquisition graph and AV's decision making

The graph-based modeling approach we adopt is essential for formalizing the distributed intersection management problem. Unlike rule-based approaches, the graph representation captures the structural relationships between vehicles and conflict zones, enabling each AV to independently reason about multi-vehicle, multi-conflict zone interactions. This formalism provides several key advantages:

(1) It enables consistent distributed decision-making without communication, as each AV constructs the same graph based on local observations;

(2) It allows formal proof of deadlock prevention (Lemma 1) and conditional guarantee of collision avoidance (Remark 3);

(3) It provides a unified framework that handles both low-inflow and high-inflow scenarios through the same underlying mechanism.

The CfDCA is designed to adapt continuously across varying levels of traffic inflow. The logic of CfDCA is governed by a graph-based model, which is independently reconstructed by each AV at every time step, using only locally sensed information. Each AV creates and maintains its own instance of this graph, with no exchange of graph representations between vehicles. The consistency of decisions across vehicles emerges from the consistent priority function and the observation that each vehicle can detect the same relative positions and approximate speeds of nearby vehicles using its own sensors.

The dynamic graph $G = (\mathcal{V}, \mathcal{E})$, where $\mathcal{V} = U \cup R$ represents the graph vertices as the union of the set of AVs $U = \{u_i\}$ as users and conflict zones $R = \{r_j\}$ as resources, and $\mathcal{E}$ denotes the set of directed edges e_{ij}. Each edge e_{ij} represents a requirement from vehicle u_i to conflict zone r_j. While each conflict zone inherently results from the interaction of AVs from two different movements, for the sake of simple indexing, we number them sequentially, ensuring each conflict zone is assigned a unique index.

Each AV independently constructs this graph by considering vehicles in proximity to the intersection and the conflict zones they require. Using the priority function, the AV determines which vehicles acquired the required conflict zones. The priority function aims to ensure an orderly and fair acquisition of conflict zones. An AV understands that it is permitted to cross the intersection only if it successfully acquires all the conflict zones required for its trajectory, and those who fail must wait until their priorities allow them to proceed.

After establishing the prerequisites for graph construction, we now proceed to describe the graph itself. The graph evolves dynamically as AVs traverse the intersection. Each AV within set $\mathcal{Q}_{\text{require}}$ is aware of the conflict zone requirements of other AVs along their paths. This awareness is achieved through local sensing and the use of pre-defined paths. However, conflict zone acquisition is restricted to AVs in set $\mathcal{Q}_{\text{acquire}}$.

For AVs in *buffer set* $\mathcal{B}$, conflict zone acquisition is not allowed. However, their requirements are still recorded to identify potential conflicts.

Example with two AVs: If an AV u_i in *buffer set* $\mathcal{B}$ requires a conflict zone r_j that has already been acquired by another AV u_k due to the higher priority, that AV must decide its next dynamic state. First, that AV measures the time in the future when it will enter the conflict zone and when the other AV exits. Second, if the entry time to conflict zone $t_{\text{entry}}(i,j)$ minus the exit time from conflict zone $t_{\text{exit}}(k,j)$ is less than the required safe gap t_{clear}, and if the requiring AV u_i is not fully stopped, it decelerates; otherwise, it accelerates unless it has already reached its maximum speed.

2.3.1 Graph-theoretic formulation

The CfDCA approach transforms the distributed optimization problem into a resource acquisition problem on a time-varying bipartite graph. At each time step t, we define a directed bipartite graph $G(t) = (\mathcal{V}, \mathcal{E}(t))$, where the vertex set $\mathcal{V} = U \cup R$ consists of vehicle vertices and conflict zone resource vertices. The edge set $\mathcal{E}(t) \subseteq U \times R$ contains directed edges $e_{ij}(t) = (u_i, r_j)$ representing a requirement from vehicle u_i to conflict zone r_j at time t.

The graph evolves according to the dynamics:

$$\mathcal{E}(t) = \{(u_i, r_j) \mid u_i \in \mathcal{Q}_{\text{require}}(t), r_j \in \mathcal{R}_i(t)\} \tag{12}$$

where $\mathcal{Q}_{\text{require}}(t)$ is the set of vehicles requiring conflict zones at time t, and $\mathcal{R}_i(t)$ is the set of conflict zones required by vehicle u_i at time t.

The resource acquisition problem can be formulated as finding a time-varying acquisition function $A(t) : R \to U \cup \{\emptyset\}$ that maps each conflict zone to at most one vehicle at any time t, such that:

$$\begin{aligned} &\text{If } A(t_{\text{entry}}(i,j), j) = u_i \text{ and } A(t_{\text{entry}}(k,j), j) = u_k \text{ with } \mathcal{M}(u_i) \neq \mathcal{M}(u_k), \text{ then:} \\ &|t_{\text{entry}}(i,j) - t_{\text{entry}}(k,j)| \geq \max(t_{\text{exit}}(i,j) - t_{\text{entry}}(i,j), t_{\text{exit}}(k,j) - t_{\text{entry}}(k,j)) + t_{\text{clear}} \end{aligned} \tag{13}$$

Eq. (13) enforces temporal safety by ensuring that when the acquisition function assigns two vehicles u_i and u_k from different movements $\mathcal{M}(u_i) \neq \mathcal{M}(u_k)$ to the same conflict zone r_j, their entry times must satisfy the safety constraint established in Eq. (2). Specifically, the temporal separation between their entries must be at least the maximum traversal time of either vehicle plus the required safety clearance time t_{clear}. This constraint directly operationalizes the safety requirement from Eq. (2) within the resource acquisition framework, ensuring that the distributed allocation process respects the fundamental collision avoidance principles by preventing conflicting vehicles from accessing the same conflict zone too closely in time.

Example with three AVs: Consider three AVs u_1, u_2, and u_3 approaching the intersection in Fig. 1(b), labeled according to the conflict zones and lane numbers shown in Fig. 1(a). Specifically, u_1 is in lane 8, u_2 is in lane 2, and u_3 is in lane 4. The conflict zone between u_1 and u_2 is denoted as r_1 in this example, while the conflict zone between u_2 and u_3 is denoted as r_2 (see Fig. 2).

Although the priority and weight mechanisms will be described in the next section, we illustrate the procedure here by assuming each AV with a nonnegative weight proceeds, whereas any AV with a negative weight decelerates. Under these conditions, vehicle u_2 maintains a nonnegative weight and thus accelerates, while u_1 and u_3 both have negative weights and must decelerate. The graph is updated at every time step, ensuring each AV reevaluates and adjusts its behavior in real time. Complex multi-vehicle consideration will be discussed in Sections 2.4 to 2.7, which is repeated at every next time step, where the evaluation is re-conducted to determine whether the conditions for acquisition have changed.

This graph-based framework is fully decentralized, enabling each AV to independently process and resolve its interactions with others using only local sensing without relying on inter-vehicle communication. Each AV infers the requirements of other AVs for conflict zones by having the knowledge of their predefined paths and determines which conflict zones are acquired by which AVs based on the priority function described in the next subsections. Since the priority of all AVs is measurable and consistent throughout the system, every AV has full knowledge of the current state of the graph at any given moment.

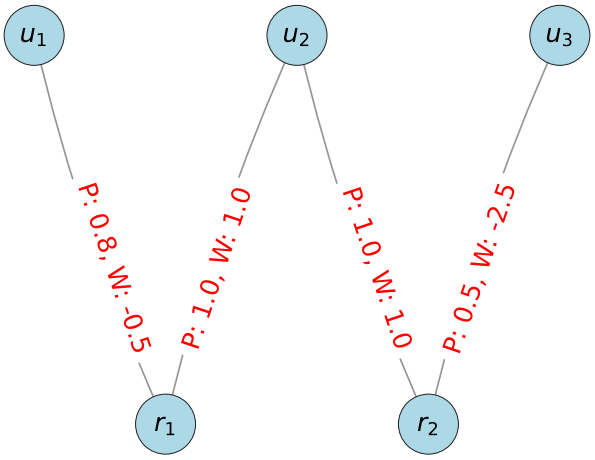

Fig. 2. An illustrative example featuring three AVs creating a graph based on CfDCA as approaching an intersection. AVs u_1, u_2, and u_3 are positioned in lanes 8, 2, and 4, respectively, as shown in Fig. 1(b). In this example, the conflict zone between u_1 and u_2 is denoted as r_1, while that between u_2 and u_3 is denoted as r_2.

2.4 AV longitudinal decision making in low-inflow regime

Let us consider an intersection with I vehicles and J conflict zones. Each conflict zone r_j receives requirements from vehicles in two conflicting movements. We define the *requirement matrix* $R \in \mathbb{R}^{J\times I}$, where:

$$R[j,i] = \begin{cases} 1, & \text{if vehicle } u_i \text{ requires conflict zone } r_j, \\ 0, & \text{otherwise.} \end{cases} \tag{14}$$

Analogously in the graph representation, each edge e_{ij} connects a vehicle vertex u_i to a conflict zone vertex r_j and represents a requirement for the conflict zone by the vehicle. The presence or absence of an edge is encoded in the requirement matrix R, where $R[j,i] = 1$ if an edge e_{ij} exists, and $R[j,i] = 0$ otherwise.

The priority function determines the order in which AVs gain acquisition to conflict zones. The priority of an AV u_i is defined as the inverse of its time-to-intersection (T):

$$p(i) = \begin{cases} \infty, & \text{if } S_{\text{LE},i} < 0, \\ \dfrac{\epsilon}{S_{\text{LE},i}}, & \text{if } v_i \le \epsilon \text{ and } S_{\text{LE},i} \ge 0, \\ \dfrac{1}{T_i}, & \text{if } v_i > \epsilon \text{ and } S_{\text{LE},i} \ge 0. \end{cases} \tag{15}$$

where $S_{\text{LE},i}$ is a signed distance to the intersection entry line, positive if u_i is upstream and negative if it has passed the line, v_i is the current speed and $T_i = \frac{S_{\text{LE},i}}{v_i}$ for positive $S_{\text{LE},i}$, and ϵ is a small threshold speed. This formulation ensures that AVs with shorter travel times to the intersection entry line are given higher priority.

Note that this priority mechanism significantly differs from a simple first-come-first-served approach. While FCFS would only consider the distance to the intersection, our priority function accounts for both distance and speed, potentially giving higher priority to faster vehicles. This distinction is crucial for optimizing intersection throughput and reducing average delay, especially in mixed-speed traffic conditions. Simulation results in Section 4 compare these approaches.

In addition, two extra matrices must be introduced. The priority matrix P assigns a numerical value to each edge according to the vehicle's priority, while the weight matrix W captures the temporal safety constraints of vehicle dynamics. Both matrices align with the graph's structure and are updated at each time step to reflect real-time conditions.

We construct the *priority matrix* $P \in \mathbb{R}^{J\times I}$, where:

$$P[j,i] = \begin{cases} p(i), & \text{if } R[j,i] = 1, \\ 0, & \text{otherwise.} \end{cases} \tag{16}$$

The vehicle with the highest priority for each conflict zone r_j gets the acquisition of the conflict zone for the time step (Acquisition: $u_k = \arg\max_i P[j,i]$).

In rare cases where two or more AVs share identical priorities, a *tie* occurs. Within the CfDCA, ties are resolved dynamically and probabilistically to prevent indefinite stalls. When a tie occurs, each tied AV independently and randomly determines whether it will assume the highest priority. Specifically, each AV randomly decides whether to consider itself as having the highest priority or not. This randomization aims to ensure that at least one AV breaks the tie and proceeds with conflict zone acquisition eventually. The

probabilistic nature of this mechanism naturally removes the tie from the system, allowing all AVs to make progress over successive time steps without requiring explicit coordination or communication.

Moreover, if a tie nonetheless remains unresolved vehicles invoke a deterministic fallback tie-breaker: they each examine their observed arrival timestamps at the Line of Consideration for all tied vehicles and assign highest priority to the vehicle with the earliest arrival. This ensures guaranteed progress in worst-case scenarios as long as AVs agree to follow CfDCA, assuming each vehicle measures arrivals of other vehicles reasonably accurately.

Finally, one can show the probability that two AVs remain tied for k successive steps decays as $(0.5)^k$, and for m AVs as $2\,(1/2^m)^k$, making extended stalemates vanishingly unlikely before vehicles clear the conflict zone and under circumstances that one vehicle is not on a trajectory to clear the conflict zone for any reason, others will stop before the intersection line of entry until they find the conflict zone cleared.

After defining the AV that gets acquisition of conflict zones, we calculate the *weight matrix* $W \in \mathbb{R}^{J\times I}$, which quantifies the temporal feasibility of each vehicle's entry into conflict zone r_j. The weight $W[j,i]$ is determined based on the relationship between the requesting AV u_i and vehicles in conflicting movement u_k, as follows:

$$W[j,i] = \begin{cases} 1, & \text{if } i = k, \\ \min_{u_k \in \mathcal{Q}_{\text{acquire}}, \mathcal{M}(u_i) \neq \mathcal{M}(u_k)} \left(t_{\text{entry}}(i,j) - t_{\text{exit}}(k,j) - t_{\text{clear}} \right), & \text{if } R[j,i] = R[j,k] = 1 \text{ and } p(u_k) > p(u_i), \\ 0, & \text{otherwise.} \end{cases} \tag{17}$$

Here, $W[j,i]$ represents the weight assigned to AV u_i for conflict zone r_j. If $i = k$, indicating that u_k is the vehicle with the highest priority that has already acquired the conflict zone, the weight is set to 1. For other vehicles u_i, the weight is calculated as the difference between the predicted entry time of u_i into the conflict zone, $t_{\text{entry}}(i,j)$, and the predicted exit time of any other vehicle from conflicting movement $M(u_k)$ in set $\mathcal{Q}_{\text{acquire}}$ with higher priority, $t_{\text{exit}}(k,j)$, minus the required safety gap t_{clear}. This condition applies only if the vehicle u_i requests the conflict zone, denoted by $R[j,i] = 1$. If these conditions are not satisfied, the weight is set to 0. This framework aims to ensure that the acquiring vehicle u_k retains the highest priority with a weight of 1, while other vehicles are evaluated based on their temporal feasibility of entering the conflict zone, respecting the safety gap t_{clear}.

Ultimately, for longitudinal decision making of each AV u_i using CfDCA, the entries in the ith column of W determine its action. The decision for AV u_i is:

$$a_i(t) = \begin{cases} a_{\max}, & \text{if } \min_j W[j,i](t) \geq 0, \\ \max(-d_{\max}, \frac{-v_i^2}{2S_{\text{LE},i}}), & \text{otherwise.} \end{cases} \tag{18}$$

where $a_i(t)$ is the acceleration of AV at time t, $a_{\max}$ is the maximum allowable acceleration, $d_{\max}$ is the maximum allowable deceleration, v_i is the AV current speed, and $S_{\text{LE},i}$ is the distance to the intersection entry line. This decision function represents vehicle u_i's solution to its local optimization subproblem of minimizing its individual delay Δt_i subject to safety constraints. The key insight is that these local optimization problems, when solved collectively using the priority and weight matrices, provide a solution to the global problem while incorporating safety constraints.

It is worth mentioning that when an AV has a leader vehicle, it must follow the minimum headway towards the leader in addition to the conflict resolution process and apply the minimum acceleration from both considerations. This aims to ensure that a vehicle accelerates (with maximum acceleration if its speed is lower than the maximum allowable speed) only if all its requirements across conflict zones are acquired (i.e., $W[j,i] > 0$ for all j), and it decelerates otherwise.

2.5 AV longitudinal decision making in high-inflow regime

The CfDCA adapts to varying traffic conditions by switching between low- and high-inflow regimes based on the number of AVs detected in the observation set. This observation set, comprising eight lanes plus the intersection space, serves as a proxy for traffic density; the more AVs present, the more conflict-zone requirements (edges) appear in the graph. To determine the threshold for changing regimes, the system examines how average delay varies with the number of AVs, identifying the point at which switching to high-inflow operations reduces overall delay.

As traffic inflow increases, the graph becomes denser and CfDCA coordinates AVs stopping positions to reduce conflicts and forming platoons for sequential crossing. In a high-inflow regime, AVs in $\mathcal{Q}_{\text{acquire}}$ proceed similarly to low-inflow mode, but those in the *buffer set* must account for potential queue discharging. If in conflicting crossing movements the headway h between the leading AV (in $\mathcal{A}$) and its follower equals the minimum value $h_{\min}$, the ego AV must decelerate before entering the *active set*. Formally, if $h \leq h_{\min}$ for a conflicting movement and $u_i \in \mathcal{B}$, then:

$$a_i = \max\left(-d_{\max}, \frac{-v_i^2}{2\,S_{\text{LC},i}} \right), \tag{19}$$

where $S_{\text{LC},i}$ is the distance to the consideration line. Otherwise, when there is no queue discharging occurring, even AVs in *buffer set* proceed similarly to low-inflow mode. This headway-based rule prevents over-saturation by halting additional conflict-zone requirements until existing queues subside. Once AVs in $\mathcal{Q}_{\text{acquire}}$ have cleared their requirements, *buffer set* vehicles may accelerate and join $\mathcal{Q}_{\text{acquire}}$, provided no other conflicts persist.

Under low-inflow conditions, AVs in the *buffer set* may enter the consideration area while decelerating if they have negative weight on their edges, stopping only as needed just before the intersection entry line. This arrangement minimizes unnecessary delays since vehicles can acquire conflict zones as soon as they reach the *active set* and resolve any temporal conflicts among different movements.

By contrast, high-inflow scenarios require AVs in the *buffer set* to stop at a point before the intersection, effectively suspending new conflict-zone requests until they join $\mathcal{Q}_{\text{acquire}}$. This restriction keeps vehicles already in the intersection area unimpeded, fosters platooning, and maximizes throughput within each movement's turn. CfDCA distinguishes low- from high-inflow operation based on vehicle density in the observation area. At each time step, the vehicle knows the total length occupied by all eight turning and through movements within a predefined observation zone, and already knows how many vehicles could fit that length under standard spacing, and counts the actual approaching vehicles. If this count exceeds 25% of the computed capacity, the mode switches to high-inflow mode and changes the stopping position of AVs; otherwise, it remains in low-inflow mode.

Remark 1 (*Tolerance Function*)**.** To prevent excessive waiting, a tolerance function is used to modify the graph weights dynamically, prioritizing AVs with longer delays. The delay tolerance $T_{\text{d}}(i)$ for AV u_i is defined as

$$T_{\text{d}}(i) = T_0 + (t_{\text{clock}}(i) - t_{\text{entry}}(i))^{\beta}, \tag{20}$$

where C is a base tolerance, β is a sensitivity parameter, $t_{\text{entry}}(i)$ is the time u_i entered the detection area, and t_{clock} is the current clock time. If the delay of u_i exceeds $T_{\text{d}}(i)$, the weights of its edges e_{ij} become positive until it enters set $\mathcal{Q}_{\text{acquire}}$, allowing u_i to proceed and gain priority.

2.6 CfDCA pseudo code

In the following, we detail the CfDCA in two parts. Algorithm 1 addresses the setup and classification of AVs approaching the intersection, including the creation of position-based subsets ($\mathcal{O}, \mathcal{A}, \mathcal{B}$) and the sets of vehicles requiring conflict zones ($\mathcal{Q}_{\text{require}}$) or eligible to acquire them ($\mathcal{Q}_{\text{acquire}}$). This classification step is crucial in determining which vehicles are actively engaged in conflict resolution and which are placed in the buffer area.

Next, Algorithm 2 presents the core logic of CfDCA: constructing the conflict-zone graph, forming the requirement matrix R, priority matrix P, and weight matrix W, and then adjusting vehicle behavior accordingly. The method accommodates varying traffic inflow levels (low and high inflow), applies a tolerance function to reduce excessive waiting times, and concludes with a fully decentralized **acceleration/deceleration** decision for each vehicle. By combining these mechanisms, CfDCA ensures collision-free intersection traversal without the need for centralized control or inter-vehicle communication.

Algorithm 1 CfDCA — Part I: Setup and Classification

Input: Local sensing data (*positions*, *speeds*) for all AVs within $D_2 + D_1$
Output: Sets $\mathcal{O}, \mathcal{A}, \mathcal{B}, \mathcal{Q}_{\text{require}}, \mathcal{Q}_{\text{acquire}}$

// Initialize all sets as empty
$\mathcal{N}, \mathcal{O}, \mathcal{A}, \mathcal{B}, \mathcal{Q}_{\text{require}}, \mathcal{Q}_{\text{acquire}} \leftarrow \emptyset$
// Define $\mathcal{N}$: vehicles not yet cleared conflict zone
$\mathcal{N} \leftarrow \{ u_i \in U \mid u_i \text{ has not cleared conflict zone} \}$
1. Classification into Position-Based Subsets:
// Here, $S_{\text{LE},i}$ is a signed distance to the intersection entry line, positive if u_i is upstream and negative if it has passed the line.
foreach *AV* $u_i \in U$ **do**
  if $S_{LE,i} \le D_2 + D_1$ **then**
    $\mathcal{O} \leftarrow \mathcal{O} \cup \{u_i\}$; /* Observation set: u_i is inside intersection or within $D_2 + D_1$ upstream of the entry line */
    if $S_{LE,i} \le D_1$ **then**
      $\mathcal{A} \leftarrow \mathcal{A} \cup \{u_i\}$; /* Active set: u_i is inside intersection or within D_1 upstream of the entry line */
$\mathcal{B} \leftarrow \mathcal{O} \setminus \mathcal{A}$; /* Buffer set: vehicles in $\mathcal{O}$ but not in $\mathcal{A}$ (still upstream) */
$\mathcal{Q}_{\text{require}} \leftarrow \mathcal{O} \cap \mathcal{N}$; /* Vehicles detected and not yet in conflict zone */
$\mathcal{Q}_{\text{acquire}} \leftarrow \mathcal{A} \cap \mathcal{N}$; /* Active vehicles (within D_1) that need a conflict zone */

2.7 CfDCA characteristics: deadlock prevention and collision avoidance

Remark 2 (*Deadlock Prevention*)**.** Deadlock is a critical challenge in decentralized systems where multiple entities compete for limited resources. In the context of CfDCA, a deadlock occurs when two or more AVs are unable to proceed due to cyclic dependencies

Algorithm 2 CfDCA — Part II: Graph, Matrices, and Acceleration

Input: Sets $\mathcal{O}, \mathcal{A}, \mathcal{B}, \mathcal{Q}_{\text{require}}, \mathcal{Q}_{\text{acquire}}$ from Part I
Output: Real-time acceleration a_i for the ego AV u_i

2. Graph and Matrix R: Create $G = (\mathcal{V}, \mathcal{E})$ with $\mathcal{V} = U \cup R$; /* Vertices: vehicles + conflict zones */
foreach *vehicle* $u_i \in \mathcal{Q}_{require}$ **do**
  Identify all conflict zones r_j on u_i's path **foreach** *required conflict zone* r_j **do**
    Add directed edge $e_{ij} = (u_i \to r_j)$ to $\mathcal{E}$ $R[j,i] \leftarrow 1$
Set $R[j,i] \leftarrow 0$ otherwise; /* If u_i does not require r_j */

3. Priority Calculation and Tie-Breaking: foreach *vehicle* $u_i \in \mathcal{Q}_{acquire}$ **do**
  if $v_i \le \epsilon$ **then**
    $p(i) \leftarrow \dfrac{\epsilon}{S_{\text{LE}_i}}$
  else
    $p(i) \leftarrow \dfrac{1}{T_i}$; /* $T_i = \dfrac{S_{\text{LE}_i}}{v_i}$ */

4. Priority Matrix P: Initialize $\mathbf{P} \in \mathbb{R}^{J \times I}$; /* J conflict zones, I vehicles */
foreach *edge* $e_{ij} = (u_i \to r_j)$ **do**
  $P[j,i] \leftarrow \text{Priority}(u_i)$
Set $P[j,i] \leftarrow 0$ if $R[j,i] = 0$

5. Weight Matrix W and Conflict Zone Acquisition: Initialize $\mathbf{W} \in \mathbb{R}^{J \times I}$ **foreach** *edge* $e_{ij} = (u_i \to r_j)$ **do**
  if u_i *has highest priority for* r_j *(i.e. already acquired)* **then**
    $W[j,i] \leftarrow 1$
  else
    $W[j,i] \leftarrow \min_{u_k \in \mathcal{Q}_{\text{acquire}},\, \mathcal{M}(u_k) \neq \mathcal{M}(u_i)} \left(t_{\text{entry}}(i,j) - t_{\text{exit}}(k,j) - t_{\text{clear}} \right)$
Set $W[j,i] \leftarrow 0$ if $R[j,i] = 0$

6. Inflow Adaptability (Low vs. High Inflow): if $|\mathcal{O}| > \mathit{threshold}$ **then**
  High-Inflow Mode: foreach *vehicle* $u_i \in \mathcal{B}$ **do**
    if *queue discharge detected on conflicting movements* ($h \le h_{\min}$) **then**
      Enforce stop/deceleration before $\mathcal{A}$ to allow clearing of platoons
else
  Low-Inflow Mode: foreach *vehicle* $u_i \in \mathcal{B}$ **do**
    Continue rolling into $\mathcal{A}$; stop only if $W[j,i] < 0$ for some j

7. Tolerance Function: foreach *vehicle* u_i *with extended waiting time* **do**
  if $((t_{clock}(u_i) - t_{entry}(u_i)) > T_d(u_i)$ **then**
    Adjust weights to favor u_i's progress if it waited too long: $W[j,i] \leftarrow$ positive value for relevant j

Final Decision (Acceleration / Deceleration): foreach *vehicle* $u_i \in \mathcal{Q}_{require}$ **do**
  if *(currentMode =* ***HIGH****)* **then**
    if $u_i \in \mathcal{B}$ ***and*** $\exists$ *conflict with* $h \le h_{\min}$ **then** /* Buffer-set vehicles check queue discharge */
      $a_i \leftarrow \max\left(-d_{\max},\ \dfrac{-v_i^2}{2\, S_{\text{LC}_i}} \right)$; // stop before $\mathcal{A}$ to avoid adding more conflict requests
  else
    if $W[j,i] \ge 0 \ \ \forall r_j$ *where* $R[j,i] = 1$ **then**
      $a_i \leftarrow a_{\max}$;
    else
      $a_i \leftarrow \max\left(-d_{\max},\ \dfrac{-v_i^2}{2\, S_{\text{LE}_i}} \right)$; // Decelerate if any $W[j,i] < 0$
return a_i ; /* Acceleration for ego AV u_i considering leader headway */

in resource acquisition, specifically conflict zones. This subsection formally defines deadlock conditions, identifies the variables involved, and demonstrates how CfDCA prevents deadlock through strict priority assignment.

Lemma 1. *A deadlock exists when there exists a closed chain of dependencies among AVs such that each AV in the chain is waiting for a conflict zone held by the next AV. In CfDCA, the strict priority order prevents deadlock.*

Proof. Assume that a deadlock occurs in CfDCA. By definition, this implies the existence of a cycle C in the dependency graph G, where:

$$|C| > 2 \quad C \cap U \neq \emptyset \quad \text{and} \quad C \cap R \neq \emptyset. \tag{21}$$

Since CfDCA enforces a strict priority order, there exists an AV $u_k \in C$ with the highest priority:

$$P(u_k) > P(u), \quad \forall u_i \in C \setminus \{u_k\}. \tag{22}$$

By the priority rule, u_k is granted access to its requested conflict zones, breaking its dependency. Consequently, the cycle C cannot exist. This contradiction proves that CfDCA prevents deadlock. □

Remark 3 (*Collision-Free Operation Logic*)**.** The CfDCA enforces strict safety conditions, dynamic priority resolution, and deadlock prevention to ensure that no two vehicles occupy the same conflict zone simultaneously.

Guarantee (under ideal assumptions). Assuming (i) perfect measurement of all vehicle states, (ii) accurate short-term trajectory prediction within the planning horizon, and (iii) that each AV can execute the computed control commands with at most a bounded actuation error, then CfDCA *guarantees* collision-free operation as follows.

To enforce collision-free operation, any two vehicles u_i, u_k from different movements requiring the same conflict zone r_j must satisfy a minimum clearance time t_{clear}, which ensures that u_i cannot enter r_j until at least t_{clear} seconds have elapsed since u_k exited that zone.

Furthermore, by construction of the dynamic weight matrix $W(t)$, whenever both vehicles are simultaneously permitted to proceed (i.e. $W[j,i](t) \geq 0$ and $W[j,k](t) \geq 0$), their assigned entry times obey

$$\left| t_{\text{entry}}(i,j) - t_{\text{entry}}(k,j) \right| \geq t_{\text{clear}} + \min(t_{\text{exit}}(i,j) - t_{\text{entry}}(i,j), t_{\text{exit}}(k,j) - t_{\text{entry}}(k,j)). \tag{23}$$

This inequality enforces temporal separation beyond the clearance time plus at least one vehicle's traversal duration, precluding overlap.

Furthermore, CfDCA presents inherent robustness to clock asynchrony between vehicles. Since the algorithm bases decisions on relative positions, speeds, and priorities rather than absolute synchronized time measurements, each vehicle's independent construction of the intersection state remains consistent despite potential temporal desynchronization.

Limitations. In reality, measurement noise, prediction error, and actuation delays can violate these ideal conditions. The above guarantee holds only if deviations remain within the assumed bounds. Results (Section 5.1) indicate that practical performance degrades under moderate sensor/actuator error.

Remark 4 (*Upper Bound Capacity*)**.** The model demonstrates that, based on current geometry, at any given time, up to two active movements can achieve full acquisition of their required conflict zones, provided that the vehicles belong to at least two non-conflicting movements. Consequently, the upper bound of the intersection's capacity in this model is twice the maximum flow of a single lane.

3 Simulation model

To evaluate, the simulation model considers an intersection with four legs that are orthogonal and symmetrical (Fig. 1(b)). Each leg has three lanes configured for right-side driving logic (Fig. 1(a)). Due to the absence of conflicts, right turns are not considered for result comparison. The car following method is the IDM model (Kesting et al., 2010; Shi and Li, 2021) with a minimum headway of one second. When an AV approaches a slower vehicle, it uses the IDM car-following model to adjust its speed to maintain a safe minimum distance from the preceding vehicle, ensuring smooth and collision-free operation. The following equations describe the IDM car-following behavior:

$$a = a_{\max}\left(1 - \left(\frac{v}{v_{\max}}\right)^{\delta} - \left(\frac{s^*(v)}{s}\right)^2\right), \tag{24}$$

where a represents acceleration (can be negative), v denotes velocity, $a_{\max}$ stands for maximum acceleration, $v_{\max}$ denotes desired velocity, δ represents the acceleration exponent (we use $\delta = 2$), s indicates the current gap to the leading vehicle, and $s^*(v)$ denotes the desired minimum gap ($h_{\min}.v$ minus the vehicle length), which depends on the vehicle speed v.

The IDM allows each AV to dynamically adjust its speed and position to maintain a safe and efficient gap from the leading vehicle. Vehicle acceleration and deceleration are modeled within realistic physical constraints. Although AVs follow predefined paths and are treated as points in the simulation, their actual dimensions are considered when assessing collision risks and ensuring safety in conflict zones.

For comparison, we use an actuated signal method that employs a variant of the max pressure approach (Varaiya, 2013), granting the green phase to the direction with the highest queue length for a minimum of 10 s. Green time dynamically extends to accommodate any remaining queue, with a maximum of 50 s.

We consider three trapezoidal traffic inflow profiles with peaks of 3600, 4800, and 7200 vehicles per hour, starting from zero and gradually reaching peak inflow in 15 min, staying at peak inflow for one hour, and decreasing to zero again in 15 min. For these scenarios, the east through and left-turn movements were assigned double the inflow of other movements to evaluate CfDCA under asymmetric traffic conditions. The performance evaluation metrics include average delay, standard deviation of delay, queue length, time gap between successive entries to conflict zones (used as a proxy for safety), and maximum throughput.

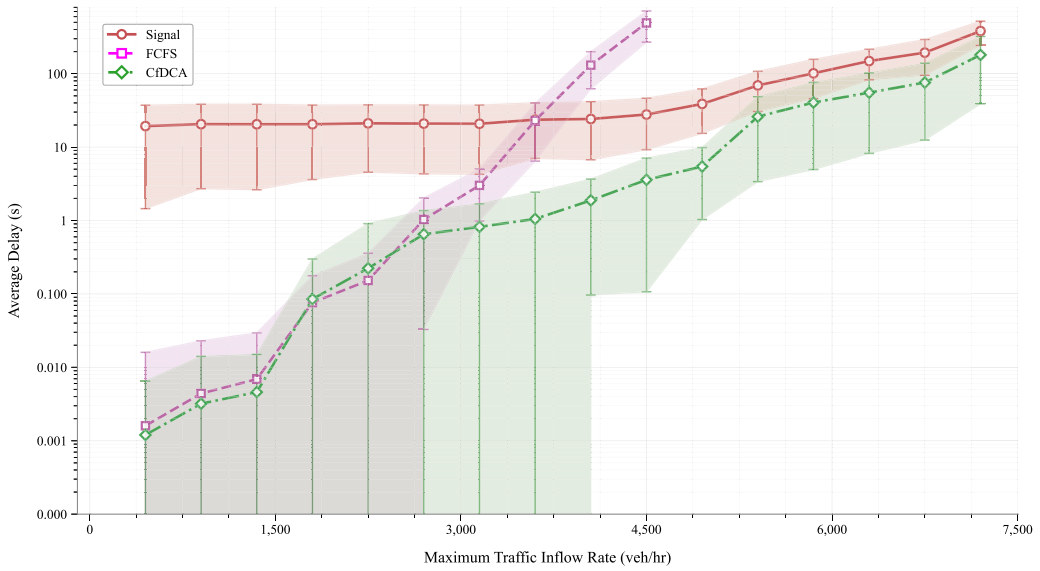

Fig. 3. Performance comparison of CfDCA, actuated signalized intersections, and FCFS approaches across varying traffic inflow rates. The logarithmic scale on the *y*-axis highlights CfDCA's superior performance at low to high inflow conditions. Error bars represent standard deviations across 6 simulation runs of each having the maximum traffic inflow rate for one hour.

4 Results

Fig. 3 presents a comprehensive performance comparison of CfDCA against actuated signalized intersections and FCFS approaches across varying traffic inflow rates with maximum from 450 to 7200 vehicles per hour. Each data point represents the average delay from 6 simulation runs, each having a trapezoidal inflow profile with the maximum inflow rate sustained for one hour. The results demonstrate CfDCA's superior performance in low to high inflow conditions, achieving lower average delays compared to both baseline methods. As inflow increases beyond 3000 veh/hr, all methods experience increased delays, with CfDCA showing competitive performance relative to actuated signalized control and substantially outperforming FCFS (which we cut the simulation after inflow of 4500 due to exponential delay increase). The following subsections provide a detailed analysis of throughput, delay distributions, queue dynamics, and safety metrics to further characterize CfDCA's operational effectiveness.

4.1 Throughput and delay estimation

Throughput is defined as the number of vehicles exiting the intersection per unit of time. By imposing a traffic inflow that exceeds the intersection capacity for the CfDCA and actuated signalized intersections, we evaluate the maximum throughput achievable within one-minute intervals. The results demonstrate that the maximum throughput values for both methods are comparable. For the signalized intersection, the maximum throughput is 835 vehicles per hour per lane (6680 vehicles per hour for eight lanes). In contrast, for CfDCA, it is 855 vehicles per hour per lane (6840 vehicles per hour for eight lanes). This finding indicates that the proposed CfDCA method maintains robustness under high-density states even without central infrastructure and communication and delivers throughput performance on par with an actuated signalized controller (Mohajerpoor et al., 2022).

For each vehicle in the simulation, we can determine the delay by comparing the actual travel time to the minimum travel time. CfDCA substantially lowers average delay and standard deviation of delay compared with actuated signal systems at lower inflow levels (Figs. 4(a) and 4(b)).

With high inflow, CfDCA demonstrates robust performance (Fig. 4(c)). The integration of platooning and the dynamic tolerance function ensures that throughput remains consistently high, comparable to the maximum capacity of a signalized intersection, close to 2-lane capacity. Furthermore, the tolerance function balances delays across different traffic movements, especially under heavy congestion.

4.2 Queue length

Figs. 5, 6, and 7 illustrate queue lengths under varying traffic conditions. Queue lengths are measured in time intervals of 60 s and shown in units of vehicles. The CfDCA consistently demonstrated shorter average queue lengths across most scenarios, particularly in low to moderate inflow conditions. For instance, in the east left turn movement for inflow with a maximum of 4800 vehicles per hour, the CfDCA maintained an average queue length of approximately 1.87 vehicles, significantly lower than the actuated signalized intersection, which averaged 8.62 vehicles.

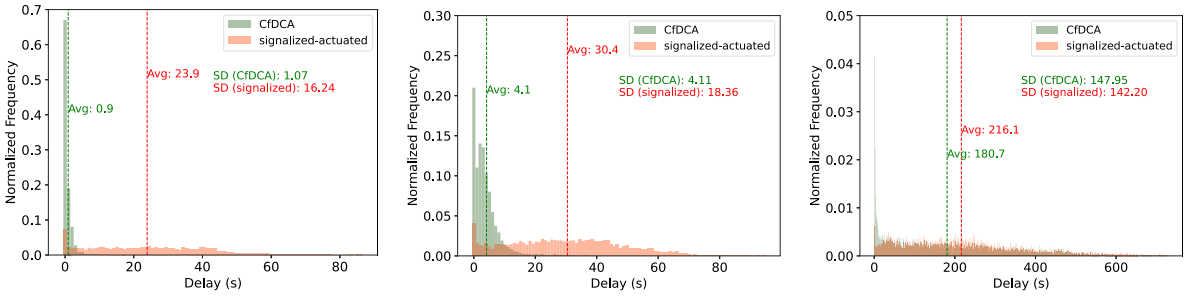

Fig. 4. Delay distribution for trapezoidal inflow with maximum rates of (a) 3600, (b) 4800, and (c) 7200 vehicles per hour. Note the different x- and *y*-axis ranges.

Under high inflow scenarios, while queue lengths naturally increased for both methods, the CfDCA still managed to maintain a more efficient flow of traffic. The adaptive nature of the CfDCA, especially its ability to switch between low-density and high-density strategies, played a key role in reducing overall queue lengths. In contrast, the actuated signalized method, despite its responsive timing cycles, often led to longer queues, particularly in scenarios with imbalanced inflow across different movements. These results underscore the effectiveness of the CfDCA in dynamically managing traffic flow, leading to reduced congestion and more efficient intersection operations.

Even in high-inflow scenarios, where two specific lanes from left to right experience double the inflow compared to others, resulting in a higher average queue length, the CfDCA method exhibits superior performance in managing queue lengths across the entire intersection. In most other lanes, the CfDCA consistently achieves shorter queue lengths compared to the actuated signalized intersections. Additionally, the adaptability of the CfDCA model is showcased through its ability to modify queue lengths by adjusting tolerance function parameters, allowing calibration for specific traffic management objectives.

The longer queues in eastbound and north left-turn movements under high-inflow conditions (Fig. 7) stem from several factors. First, eastbound flows have double the inflow of other movements, and their conflicts with the north left turn lead to spillbacks. Second, CfDCA's platooning strategy (Section 2.5) implicitly prioritizes and groups vehicles by movement, creating temporary queues to boost overall throughput. Third, the priority–tolerance tradeoff in CfDCA can extend queues for movements conflicting with high-volume flows. In contrast, actuated signals adjust green time based on detected queues, often reducing peak queue lengths at the cost of higher average delay and lower throughput. This illustrates a core tradeoff: CfDCA prioritizes total throughput and average delay, while actuated signals may minimize maximum queues for specific movements.

4.3 Comparison with first-come-first-served approach

To further evaluate the effectiveness of our proposed CfDCA, we compare its performance against the FCFS approach, which is commonly used as a baseline in intersection management studies. In the FCFS implementation, vehicles acquire conflict zones based solely on their arrival order at the intersection, without considering speed or other factors in prioritization.

While Fig. 3 provides a broad range comparison between CfDCA and FCFS, Fig. 8 illustrates the difference in delay distributions between CfDCA and FCFS for the 3600 vehicles per hour inflow scenario. Even at this relatively low inflow level, the FCFS approach results in significantly higher delays (average: 23.7 s, standard deviation: 28.09 s) compared to CfDCA (average: 0.9 s, standard deviation: 1.07 s).

This substantial performance gap highlights the critical role of CfDCA's prioritization mechanism that considers both distance and speed, rather than simply arrival order. The FCFS approach fails to efficiently manage intersection resources because it does not account for vehicle dynamics or optimize for throughput, resulting in inefficient sequencing decisions that compound delays across vehicles.

Furthermore, the large standard deviation in the FCFS results indicates inconsistent performance and poor predictability, while CfDCA's small standard deviation demonstrates highly consistent performance across all vehicles. The performance degradation of FCFS would become even more pronounced at higher inflow levels, as the inefficient resource allocation/acquisition would lead to growing queues and potentially gridlock scenarios.

This detailed comparison complements the comprehensive performance evaluation presented in Fig. 3, which demonstrates CfDCA's consistent superiority over FCFS across almost all traffic inflow levels.

4.4 Safety

CfDCA enforces a minimum clearance time of 1 s for conflict zones between vehicles that occupy them. To evaluate safety, we examined vehicles with conflicting paths that pose a risk of collision by successive entries to a conflict zone. We measured the time gap between their entry into the conflict zone. We determined the minimum and average time gaps by analyzing all conflict zones

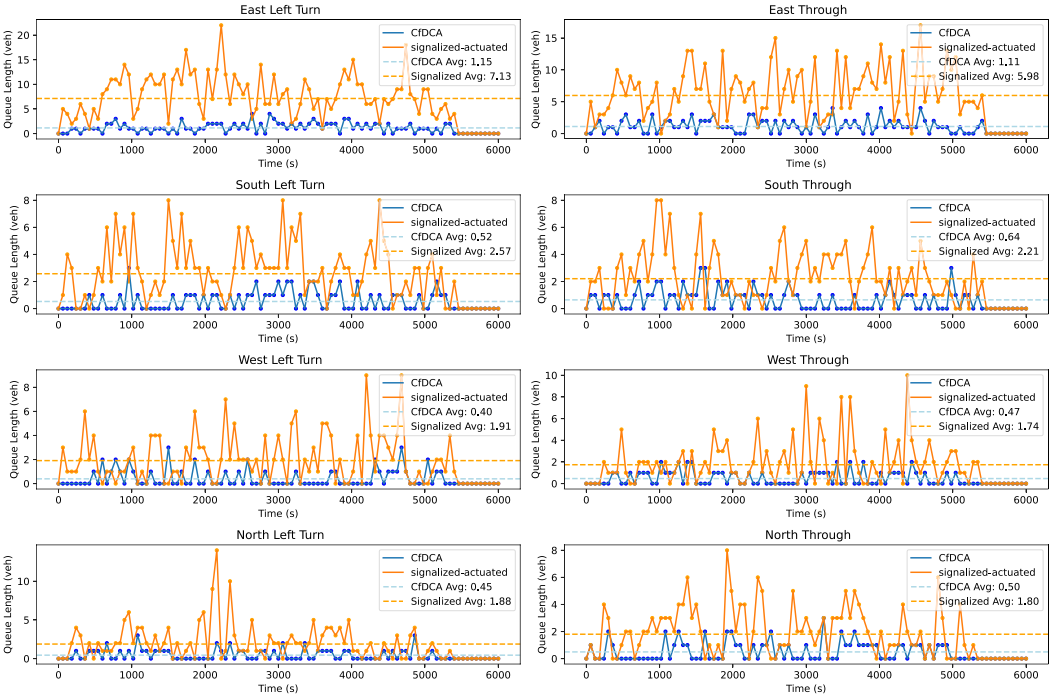

Fig. 5. The queue lengths for different traffic movements with the inflow scenario of 3600 vehicles per hour, measured every minute. The CfDCA method demonstrates significantly smaller queue lengths compared to actuated signalized intersections.

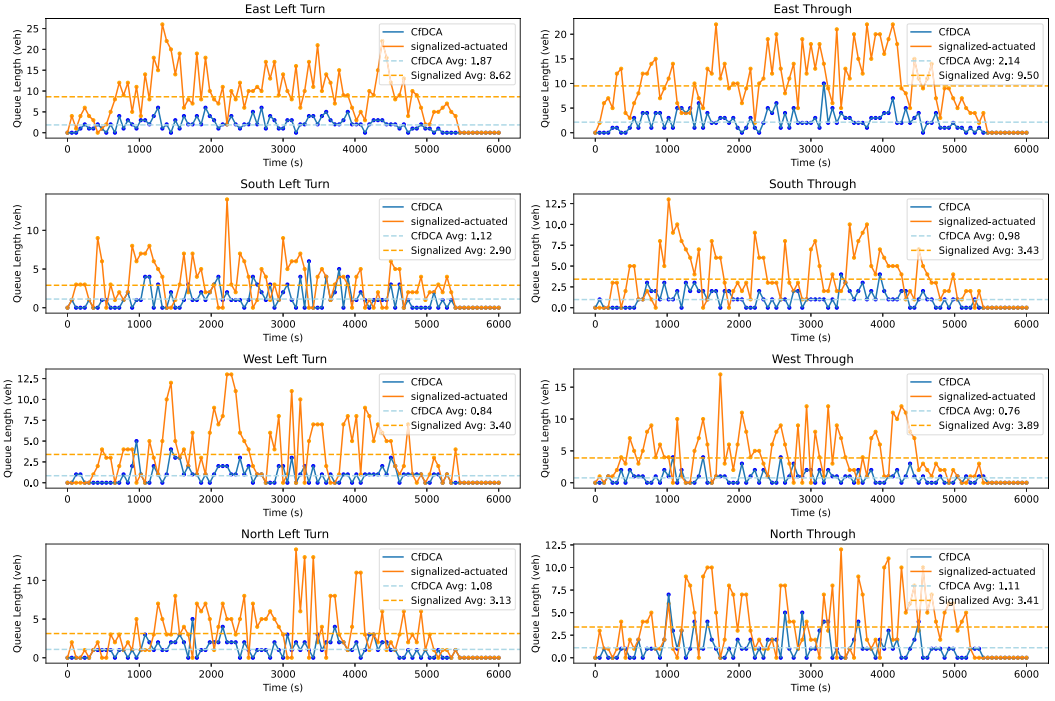

Fig. 6. The queue lengths for various traffic movements with the inflow scenario of 4800 vehicles per hour, measured every minute. The CfDCA method maintains smaller queue lengths in all lanes, showcasing its efficiency even as inflow increases.

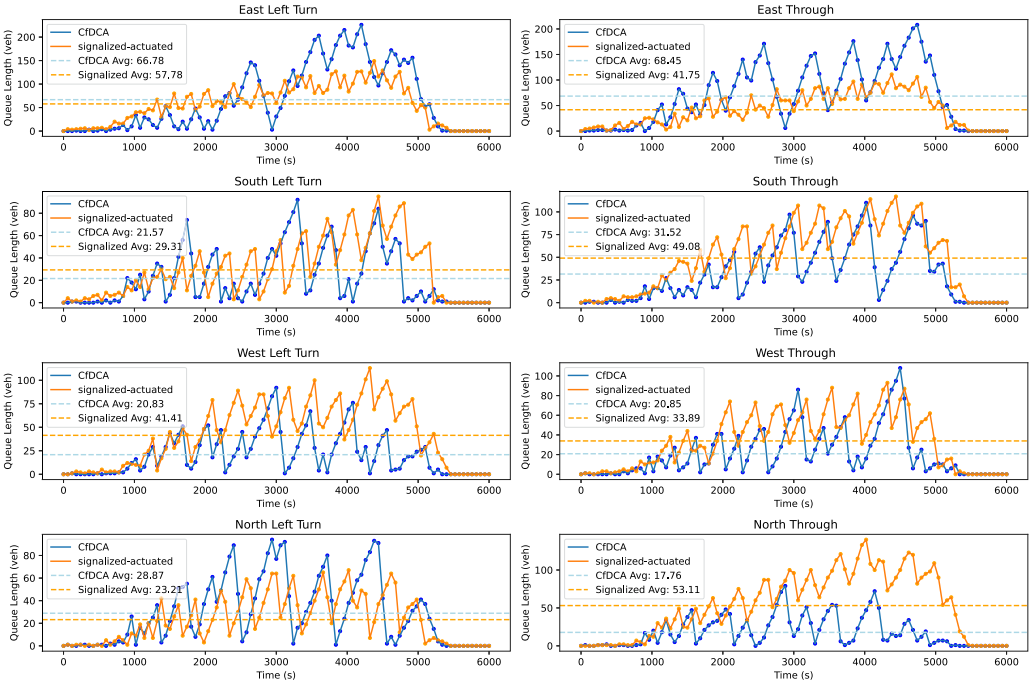

Fig. 7. The queue lengths for different traffic movements with the high-inflow scenario of 7200 vehicles per hour, measured every minute. While the queue lengths increase in lanes with double the inflow, the CfDCA method outperforms actuated signalized intersections in terms of overall traffic management.

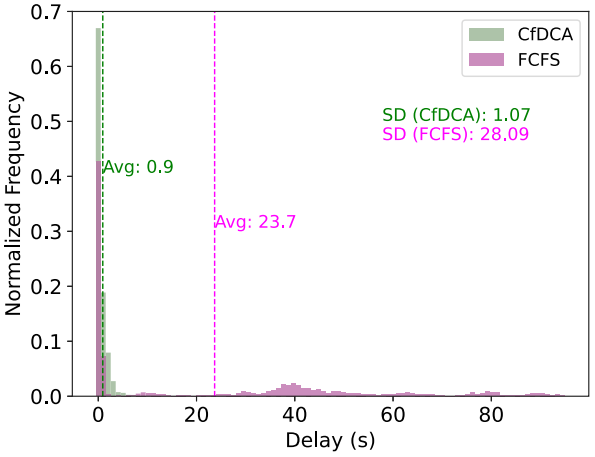

Fig. 8. Delay distribution comparison between CfDCA and FCFS for the 3600 vehicles per hour inflow scenario. Note the substantially lower and more consistent delays achieved by CfDCA.

Table 2
Potential conflicts time gaps with the CfDCA for trapezoidal inflow profiles.

Peak inflow (veh/h)	Minimum conflict gap (s)	Average conflict gap (s)
3600	1.55	7.36
4800	1.59	10.32
7200	1.59	30.65

across various inflow profiles (see Table 2). Our method aims to ensure safety by maintaining a minimum time gap of 1 s. This includes the first AV passing through the conflict zone, followed by a minimum clearance time. The table shows that the average time gap increases with higher inflow, likely due to more frequent instances of platooning.

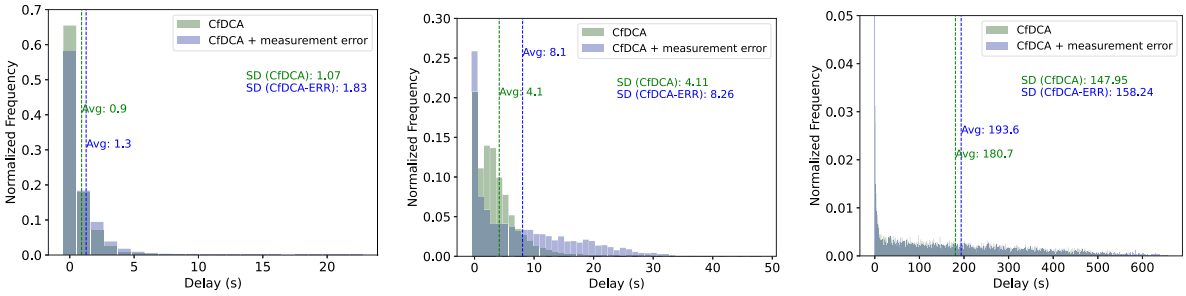

Fig. 9. Impact of measurement errors on delay distribution for trapezoidal inflow profiles with maximum rates of (a) 3600, (b) 4800, and (c) 7200 vehicles per hour. With realistic sensor errors (1.0 m position error, 0.5 m/s speed error), CfDCA maintains robust performance with moderate increases in delay.

5 Discussion

Ensuring robust and efficient intersection management goes hand in hand with addressing real-world complexities, such as sensing inaccuracies and the presence of diverse road users. This section discusses the influence of measurement errors on the proposed CfDCA, demonstrating how temporary disruptions may occur but can be mitigated through responsive adjustments in vehicle behavior. Additionally, we discuss extensions to accommodate emergency vehicles, pedestrians, and cyclists, emphasizing how CfDCA upholds safety and efficiency across various traffic scenarios.

5.1 Impact of measurement errors on CfDCA

While decentralized and communication-free, CfDCA relies on each AV's accurate sensing and prediction to build vehicle–conflict-zone interaction graphs. Real-world errors in position, speed, or trajectory measurements can impair its performance. The sensor-error model from Elmquist and Negrut (2020) uses Gaussian noise that varies with detection conditions. We add noise with standard deviation 1.0 (m) to position and 0.5 (m/s) to speed measurements to mimic typical AV sensor performance.

To evaluate CfDCA's robustness to measurement errors, we simulated Gaussian noise on position and speed across three inflow scenarios; Fig. 9 illustrates the resulting impacts on delay distributions.

Measurement-error impacts vary across inflow levels, in low-inflow (3600 vehicles/h), mean delay increases from 0.9 (s) to 1.3 (s) (44%); in medium-inflow (4800 vehicles/h), near the transition threshold between low- and high-inflow regimes, it almost doubles from 4.1 (s) to 8.1 (s) (97%); and in high-inflow (7200 vehicles/h), it rises from 180.7 (s) to 193.6 (s) (7%).

Simulation results highlight:

- **Inflow sensitivity:** error impact is highest at medium inflow, moderate at low inflow, and minimal at high inflow.
- **Safety:** no collisions occurred under all error conditions, confirming robust safety.
- **Performance:** CfDCA outperforms actuated signal control in every scenario despite measurement errors.

Measurement errors can cause transient deviations from optimal decisions, but CfDCA's continuous updates correct them in the next time step, and reduced inter-vehicle distances near the intersection lessen position-error effects, preserving decision accuracy in critical zones. CfDCA remains robust under realistic measurement errors, confirming its practical viability for real-world AV systems. Maintaining safe operation despite sensor inaccuracies is essential for any deployable autonomous intersection management solution. It is important to note that as AVs approach the intersection and come closer to one another, the relative measurement errors tend to decrease due to improved sensor accuracy at shorter ranges (an effect not incorporated in our current simulation model). This natural error reduction mitigates the likelihood of significant disruptions to the CfDCA protocol in the critical areas near the intersection.

5.2 Consideration of emergency vehicles, public transit, pedestrians, cyclists, and mixed traffic

The CfDCA has the potential to adapt to diverse traffic users, including emergency vehicles, public transit, pedestrians, and cyclists, and remains robust against vehicles that deviate from it, ensuring safety and efficiency under various scenarios. This subsection outlines the strategies for incorporating these users into the CfDCA framework.

5.2.1 Emergency vehicles and public transit

Emergency vehicles, such as ambulances, police, or fire trucks, and public transit vehicles such as buses or trams require prioritized access to intersections to minimize delays. The CfDCA algorithm can accommodate this by assigning emergency and public transit vehicles the highest priority upon detection, ensuring full acquisition of all required conflict zones for a seamless crossing. Specifically:

- **Queue Clearance:** If an emergency vehicle or bus encounters a queue at the intersection, its presence allows the vehicles in front of the queue to temporarily consider themselves as having higher priority. This forces other vehicles to stop and clears the path for the priority vehicle.
- **Alternative Approach:** In cases where immediate access to the intersection is needed, emergency and transit vehicles can use right-turn lanes, which typically have fewer or no conflict zones, to approach the intersection. Upon reaching the intersection, the CfDCA algorithm prioritizes the relevant vehicle, stopping all other movements to allow its crossing.

These strategies ensure that emergency vehicles and public transit can navigate intersections with minimal delay, leveraging the CfDCA's dynamic prioritization mechanisms.

5.2.2 Pedestrians and cyclists

Pedestrians and cyclists are treated as vulnerable users with absolute priority in the CfDCA framework. The algorithm is equipped to detect their presence and adapt vehicle behaviors to ensure safety:

- **Pedestrian Crossings:** Pedestrian areas, such as crosswalks, can be defined as zones where AVs must stop when pedestrians are detected. To facilitate safe crossings, pathways can be segmented into smaller areas (e.g., median islands) on multilane roads, providing AVs time to adjust their behavior for approaching pedestrians. This segmented crossing approach minimizes disruptions to traffic flow while ensuring pedestrian safety.
- **Cyclists:** Cyclists are considered lane users with absolute priority. When cyclists are detected in a lane or near a conflict zone, AVs yield to them, ensuring their safe and uninterrupted passage. The CfDCA algorithm dynamically incorporates cyclists into the priority system, treating them as critical road users.

The presence of pedestrians and cyclists introduces additional delays to the system, which is expected given their absolute priority.

- **Signalized Control for Pedestrians and Cyclists:** In high-inflow scenarios, signal systems can be introduced to organize pedestrian and cyclist crossings, reducing their impact on vehicular flow, and the system can also benefit from a pedestrian scramble phase, which allows pedestrians to cross the intersection in all directions, including diagonally, while vehicles are stopped on all approaches simultaneously. Pedestrians would be no worse off than existing traffic signal controlled intersections, but would suffer more delay than if at unsignalized intersections and given right-of-way on demand.

5.2.3 Mitigating non-compliant vehicles

If one or more vehicles deviate from CfDCA, due to aggressiveness, malicious intent, or sensor or decision errors, the continuously updated resource-acquisition graph detects noncompliance in real time. AVs have the potential to adopt safe fallback behaviors, yielding right-of-way to the violator. Future research should address mitigation and enforcement mechanisms.

5.2.4 Mixed traffic and human-driven vehicles

One imagines at a non-centrally controlled and communication-free intersection, human-driven vehicles would generally adhere to a FCFS scheme while AVs continue to coordinate via CfDCA. AVs detect and classify human drivers as non-compliant, and potentially FCFS agents, accounting for larger reaction times and headways, and yield whenever a human has already claimed the next conflict zone. AV–AV interactions remain governed by the CfDCA, whereas AV–human and human–human encounters follow FCFS rules (Mohajerpoor and Ramezani, 2019). To guard against deadlocks arising from the combination of CfDCA and FCFS claims, a temporary FCFS grant may be conferred to human drivers to restore movement, after which AVs re-synchronize using the standard CfDCA protocol. Note that this integration is purely conceptual and has not been implemented in the present work; it serves only to illustrate one possible approach to accommodating human drivers in a CfDCA-managed environment.

5.3 Architectural benefits of CfDCA's distributed design

CfDCA demonstrates that fully distributed intersection management can achieve near-optimal throughput of 6840 veh/h, or 95% of the theoretical 7200 veh/h (1-s headway), while eliminating the need for communication infrastructure and centralized control.

CfDCA forms vehicle platoons under high inflow via purely local decisions as its priority function and tolerance mechanism group same-movement vehicles to maximize throughput and prevent conflicts. Rather than fixed first-come, first-served rules, CfDCA shifts from individual optimization at low inflow to platoon-forming behavior as traffic increases.

A key feature of CfDCA is deadlock prevention without centralized coordination, by strict priority ordering, as proved in Lemma 1, the highest-priority vehicle always secures its required conflict zones, eliminating cyclic dependencies and ensuring robust distributed operation.

The distributed design of CfDCA delivers key advantages:

- **Resilience:** No single point of failure, so operation continues despite individual vehicle sensor or processing faults.
- **No communication dependency:** Avoids network degradation, latency, and security vulnerabilities.
- **Manufacturer independence:** Any AV vendor can adopt the priority protocol without standardized communication hardware.
- **Computational scalability:** Processing grows linearly with vehicle count, unlike the exponential complexity of centralized schemes.

As AVs move towards independent decision-making, CfDCA uses onboard sensing and computation to achieve near-optimal collective performance.

5.4 Extending CfDCA to complex intersection geometries

CfDCA performs strongly in our simulation and applies to any intersection with defined entry lines and conflict zones; tests on a generic four-legged intersection with multiple movement types support its broader applicability. As noted in Section 2.1, we assume lane discipline with predetermined paths for clarity. For shared lanes permitting multiple trajectories from one approach (e.g., straight and right turns), CfDCA can be extended via:

- **Dynamic conflict zone identification**: adapt the graph in real time using observed turn indicators and vehicle positions to assign conflict zones.
- **Conventional signaling integration**: use existing turn signals as intent cues to predict routes without electronic communication.
- **Expanded conflict zone mapping**: include all potential conflict zones for multi-trajectory approaches until a vehicle's actual path is clear.

These extensions preserve CfDCA's core strength — conflict resolution via local decision-making without communication — and its resource-acquisition graphs, priority-based decision-making, and deadlock prevention apply to any intersection, given appropriately defined conflict zones. CfDCA's generalizable principles provide a robust framework for managing diverse intersection geometries, including complex layouts beyond the four-way design tested in our simulations.

6 Conclusions

This paper presents a *Communication-free Distributed Control Algorithm* (CfDCA) to manage AV at intersections without relying on centralized control or communication systems. CfDCA demonstrates its effectiveness in enhancing traffic efficiency and safety by dynamically adjusting to different traffic inflow levels and employing a combination of distance- and priority-based control mechanisms. By integrating a dynamic graph-based framework, CfDCA effectively models the interactions between AVs and conflict zones, enabling precise and scalable intersection management and demonstrates collision avoidance and prevents deadlocks by design, without the need for centralized control or communication. The algorithm excels in reducing average delays and maintaining high throughput, particularly in low to moderate-inflow scenarios, where it outperforms actuated signalized intersections, and a first-come-first-served strategy. Additionally, CfDCA's aims to ensure robust safety measures through a minimum clearance time in conflict zones, preventing collisions. Even with realistic sensor measurement errors, CfDCA maintains stable operation with only modest increases in delay, demonstrating resilience to noisy data. The simulation results demonstrate the algorithm's effectiveness in handling complex traffic conditions, making it a viable approach.

To further test CfDCA's performance and address potential real-world challenges, we plan to implement this method on reduced-scale mobile robots (RSMRs) in a controlled environment. RSMRs provide a cost-effective and flexible platform for testing autonomous driving algorithms in physical settings, overcoming many of the limitations associated with full-scale vehicle testing (Tuchner and Haddad, 2017; Levy and Haddad, 2022; Xie et al., 2024). This future work will enable us to refine the CfDCA method based on empirical data, ensuring its readiness for real-world deployment. Future research should address the challenges by considering the inclusion of pedestrians, emergency vehicles, and scenarios where not all AVs adhere to CfDCA. Additionally, exploring the method's feasibility and effectiveness at a network level is a research priority.

CRediT authorship contribution statement

Alireza Soltani: Writing – review & editing, Writing – original draft, Visualization, Validation, Software, Methodology, Investigation, Formal analysis, Data curation, Conceptualization. **David M. Levinson:** Writing – review & editing, Writing – original draft, Supervision, Project administration, Methodology, Investigation, Funding acquisition, Formal analysis, Conceptualization. **Mohsen Ramezani:** Writing – review & editing, Writing – original draft, Validation, Supervision, Project administration, Methodology, Investigation, Funding acquisition, Formal analysis, Conceptualization.

Acknowledgments

This research was partially funded by the Australian Research Council, Australia [grant number DP220100882]. The authors thank Arman Haghbayan for his valuable comments on the presentation of the manuscript.

References

Carlino, D., Boyles, S.D., Stone, P., 2013. Auction-based autonomous intersection management. In: 16th International IEEE Conference on Intelligent Transportation Systems. ITSC 2013, IEEE, pp. 529–534.

Chen, L., Valadkhani, A.H., Ramezani, M., 2021. Decentralised cooperative cruising of autonomous ride-sourcing fleets. Transp. Res. Part C: Emerg. Technol. 131, 103336.

Di, X., Shi, R., 2021. A survey on autonomous vehicle control in the era of mixed-autonomy: From physics-based to AI-guided driving policy learning. Transp. Res. Part C: Emerg. Technol. 125, 103008.

Dresner, K., Stone, P., 2008. A multiagent approach to autonomous intersection management. J. Artificial Intelligence Res. 31, 591–656.

Elmquist, A., Negrut, D., 2020. Methods and models for simulating autonomous vehicle sensors. IEEE Trans. Intell. Veh. 5 (4), 684–692.

Gholamhosseinian, A., Seitz, J., 2022. A comprehensive survey on cooperative intersection management for heterogeneous connected vehicles. IEEE Access 10, 7937–7972.

Hao, Y., Chung, H., Vu, H.L., 2024. Integrating local planners into autonomous intersection management: Bridging global planning and dynamic execution. IEEE Trans. Intell. Veh..

Hao, R., Zhang, Y., Ma, W., Yu, C., Sun, T., van Arem, B., 2023. Managing connected and automated vehicles with flexible routing at "lane-allocation-free" intersections. Transp. Res. Part C: Emerg. Technol. 152, 104152.

He, Z., Zheng, L., Lu, L., Guan, W., 2018. Erasing lane changes from roads: A design of future road intersections. IEEE Trans. Intell. Veh. 3 (2), 173–184.

Kamal, M.A.S., Imura, J.-i., Hayakawa, T., Ohata, A., Aihara, K., 2014. A vehicle-intersection coordination scheme for smooth flows of traffic without using traffic lights. IEEE Trans. Intell. Transp. Syst. 16 (3), 1136–1147.

Kesting, A., Treiber, M., Helbing, D., 2010. Enhanced intelligent driver model to access the impact of driving strategies on traffic capacity. Philos. Trans. R. Soc. A: Math., Phys. Eng. Sci. 368 (1928), 4585–4605.

Lee, J., Park, B., 2012. Development and evaluation of a cooperative vehicle intersection control algorithm under the connected vehicles environment. IEEE Trans. Intell. Transp. Syst. 13 (1), 81–90.

Levin, M.W., Fritz, H., Boyles, S.D., 2016. On optimizing reservation-based intersection controls. IEEE Trans. Intell. Transp. Syst. 18 (3), 505–515.

Levin, M.W., Rey, D., 2017. Conflict-point formulation of intersection control for autonomous vehicles. Transp. Res. Part C: Emerg. Technol. 85, 528–547.

Levy, R., Haddad, J., 2022. Cooperative path and trajectory planning for autonomous vehicles on roads without lanes: A laboratory experimental demonstration. Transp. Res. Part C: Emerg. Technol. 144, 103813.

Li, Z., Chitturi, M.V., Zheng, D., Bill, A.R., Noyce, D.A., 2013. Modeling reservation-based autonomous intersection control in VISSIM. Transp. Res. Rec. 2381 (1), 81–90.

Li, L., Wang, F.-Y., 2006. Cooperative driving at blind crossings using intervehicle communication. IEEE Trans. Veh. Technol. 55 (6), 1712–1724.

Mahmassani, H.S., 2016. 50Th anniversary invited article—Autonomous vehicles and connected vehicle systems: Flow and operations considerations. Transp. Sci. 50 (4), 1140–1162.

Makarem, L., Gillet, D., 2011. Decentralized coordination of autonomous vehicles at intersections. IFAC Proc. Vol. 44 (1), 13046–13051.

Makarem, L., Gillet, D., 2012. Fluent coordination of autonomous vehicles at intersections. In: 2012 IEEE International Conference on Systems, Man, and Cybernetics. SMC, IEEE, pp. 2557–2562.

Malekzadeh, M., Papamichail, I., Papageorgiou, M., Bogenberger, K., 2021. Optimal internal boundary control of lane-free automated vehicle traffic. Transp. Res. Part C: Emerg. Technol. 126, 103060.

Medina, A.I.M., Creemers, F., Lefeber, E., van de Wouw, N., 2019. Optimal access management for cooperative intersection control. IEEE Trans. Intell. Transp. Syst. 21 (5), 2114–2127.

Mirheli, A., Tajalli, M., Hajibabai, L., Hajbabaie, A., 2019. A consensus-based distributed trajectory control in a signal-free intersection. Transp. Res. Part C: Emerg. Technol. 100, 161–176.

Mohajerpoor, R., Cai, C., Ramezani, M., 2022. Optimal traffic signal control of isolated oversaturated intersections using predicted demand. IEEE Trans. Intell. Transp. Syst. 24 (1), 815–826.

Mohajerpoor, R., Ramezani, M., 2019. Mixed flow of autonomous and human-driven vehicles: analytical headway modeling and optimal lane management. Transp. Res. Part C: Emerg. Technol. 109, 194–210.

Mohebifard, R., Hajbabaie, A., 2021. Connected automated vehicle control in single lane roundabouts. Transp. Res. Part C: Emerg. Technol. 131, 103308.

Naderi, M., Papageorgiou, M., Troullinos, D., Karafyllis, I., Papamichail, I., 2023. Controlling automated vehicles on large lane-free roundabouts. IEEE Trans. Intell. Veh. 9 (1), 3061–3074.

Naderi, M., Typaldos, P., Papageorgiou, M., 2025. Lane-free signal-free intersection crossing via model predictive control. Control Eng. Pract. 154, 106115.

Rios-Torres, J., Malikopoulos, A.A., 2016. A survey on the coordination of connected and automated vehicles at intersections and merging at highway on-ramps. IEEE Trans. Intell. Transp. Syst. 18 (5), 1066–1077.

Shi, X., Li, X., 2021. Empirical study on car-following characteristics of commercial automated vehicles with different headway settings. Transp. Res. Part C: Emerg. Technol. 128, 103134.

Tuchner, A., Haddad, J., 2017. Vehicle platoon formation using interpolating control: A laboratory experimental analysis. Transp. Res. Part C: Emerg. Technol. 84, 21–47.

Varaiya, P., 2013. Max pressure control of a network of signalized intersections. Transp. Res. Part C: Emerg. Technol. 36, 177–195.

Xie, Z., Ramezani, M., Levinson, D., 2024. Reduced-scale mobile robots for autonomous driving research. IEEE Trans. Intell. Transp. Syst. 25 (11), 15367–15387.

Yang, K., Guler, S.I., Menendez, M., 2016. Isolated intersection control for various levels of vehicle technology: Conventional, connected, and automated vehicles. Transp. Res. Part C: Emerg. Technol. 72, 109–129.

Yu, C., Sun, W., Liu, H.X., Yang, X., 2019. Managing connected and automated vehicles at isolated intersections: From reservation-to optimization-based methods. Transp. Res. Part B: Methodol. 122, 416–435.